

# A Magnetic Field-enriched Surface-enhanced Resonance Raman Spectroscopy Strategy Towards the Early Diagnosis of Malaria

Clement Yuen, Quan Liu\*

Division of Bioengineering, School of Chemical and Biomedical Engineering, Nanyang Technological University, Singapore 637457

## ABSTRACT

Early malaria diagnosis is important because malaria disease can develop into fatal illness within hours upon the appearance of the first symptom. The low concentration of the diagnosis biomarker, hemozoin, at the early stage of malaria disease makes early diagnosis difficult. In this paper, we present a magnetic field-enriched surface-enhanced resonance Raman spectroscopy (SERRS) strategy for the sensitive detection of  $\beta$  – hematin crystals, which is equivalent to hemozoin in the characteristics of Raman spectrum, by using magnetic nanoparticles. We observe several orders of magnitude enhancement in the SERRS signal of enriched  $\beta$  – hematin in comparison to the Raman signal of  $\beta$  – hematin in the cases of SERRS alone or magnetic enrichment alone, showing the great potential of this method towards early malaria diagnosis.

**Keywords:** Hemozoin, Raman spectroscopy, surface-enhanced Raman scattering, resonance Raman, hematin, malaria, magnetic nanoparticles.

## 1. INTRODUCTION

Human malaria disease is a worldwide disease.<sup>1</sup> Early diagnosis is critical to reducing morbidity and mortality rates since fatal illness can be resulted within hours after the development of the first malaria disease symptom.<sup>2</sup> In malaria diagnosis, Raman spectroscopy has shown great potential for the detection of a malaria biomarker, hemozoin.<sup>3</sup> Compared to blood smear examination, which is the current “gold standard” method, Raman diagnosis is faster and less labor-intensive; moreover, it requires minimal expertise for data interpretation.<sup>4</sup> However, one significant disadvantage of Raman spectroscopy is the intrinsically weak Raman signal,<sup>5</sup> which is aggravated by the low concentration of the malaria diagnosis biomarker at the early stage of malaria infection.<sup>6</sup>

In this paper, we propose a magnetic field-enriched surface-enhanced resonance Raman spectroscopy (SERRS) strategy to enrich the  $\beta$  – hematin crystals, which is equivalent to hemozoin in the characteristics of Raman spectra,<sup>7</sup> by using  $\text{Fe}_3\text{O}_4@Ag$  nanoparticles to enhance the SERRS signal. We will also compare the different Raman strategies for the detection of  $\beta$  – hematin crystals: 1) magnetic field-enriched SERRS, 2) SERRS, 3) magnetic field-enriched RRS, and 4) RRS to demonstrate the potential for integrating SERRS and magnetic enrichment for the sensitive detection of hemozoin towards early malaria diagnosis.

## 2. MATERIALS AND METHODS

### 2.1 Synthesis of $\beta$ – hematin crystals

An acid-catalyzed method was used to fabricate the  $\beta$  – hematin crystals.<sup>8</sup> 7.9 mM of Ferriprotoporphyrin IX chloride was dissolved in a 0.1-M NaOH solution under constant heating at 60 °C and stirring at 150 rpm. After 10 min and 14 min, 1.45 ml of HCl (1 M) and 8.825 ml of acetate solution were mixed into the solution, respectively. The heating was continued for another 46 min, after which the heating and stirring were stopped, and the mixture was left undisturbed in a dark environment for 24 h. Finally, the solute was washed with methanol and then by deionized water. The solute was collected by filtration with 0.2  $\mu\text{m}$  supor filter and dried at room temperature over  $\text{P}_2\text{O}_5$  for 48 h.

\* quanliu@ntu.edu.sg; phone +65 6513-8298; fax +65 6791-1761 <http://www3.ntu.edu.sg/home/quanliu/>

## 2.2 Fabrication of Fe<sub>3</sub>O<sub>4</sub>@Ag magnetic nanoparticles

The nanoparticles with iron oxide core and silver shell were synthesized by using the seed-growth reduction method.<sup>9, 10</sup> A mixture of Fe<sub>3</sub>O<sub>4</sub> nanoparticles at concentration of 16.2 mM in 20 ml of ethanol was added drop-wise to ethanol (80 ml) with polyacrylic acid (0.15 g), prior to the sonication of the mixture for 15 min. Subsequently, the Fe<sub>3</sub>O<sub>4</sub> nanoparticles were collected by using a magnet and washed with ethanol. A mixture of deionized water and ethanol (19.4:80.6: % v/v) with 2.8-mM AgNO<sub>3</sub> was used to re-disperse Fe<sub>3</sub>O<sub>4</sub> nanoparticles (2.1 mM) in an ultrasonic bath for 30 min. Then, 4.1 mM of hydroxylamine hydrochloride and 8.1 mM NaOH in triton X-100, ethanol and deionized water (9.0:70.8:28.3% v/v/v) was added drop-wise (5.88 μl/sec) to the suspension of Fe<sub>3</sub>O<sub>4</sub> nanoparticles to reduce the adsorbed Ag<sup>+</sup> salt. Finally, 19.4 mM of AgNO<sub>3</sub> in triton X-100, ethanol and deionized water (2:65.3:32.7% v/v/v) was added drop-wise (5.88 μl/sec) to the mixture. This second AgNO<sub>3</sub> addition was to ensure growth of Ag on the Ag seeds formed on the Fe<sub>3</sub>O<sub>4</sub> core at the first introduction of AgNO<sub>3</sub>. The Fe<sub>3</sub>O<sub>4</sub> nanoparticles were collected using a magnet, washed, suspended in ethanol (15 ml) and followed by the filtering with 0.2-μm support filters.

## 2.3 Raman Instrumentation

All samples were analyzed using an inVia Renishaw Raman system with 633-nm excitation wavelength. Excitation power of 10 mW for ordinary Raman spectroscopy and 0.1 mW for SERS study of R6G and β-hematin at different concentrations.

## 2.4 Field emission scanning electron microscope (FESEM) analysis

The nanoparticles and β-hematin were imaged with a JOEL JSM-6700F field emission scanning electron microscope (FESEM) with an acceleration voltage of 5 kV.

# 3. RESULTS

Figure 1 shows the field emission scanning electron microscope (FESEM) image of fabricated β-hematin crystals. These β-hematin crystals have sizes comparable to that of the hemozoin biocrystals reported in the literature.<sup>11</sup> Hence, similar SERRS enhancement effect would be resulted in the two different types of crystals due to the close resemblance in the spatial dimensions.

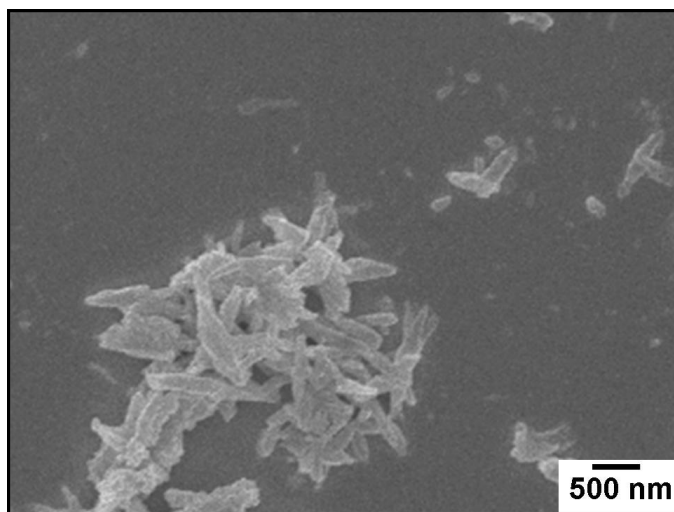


Figure 1. FESEM image of β-hematin crystals.

Figure 2(a) gives FESEM image of the raw  $\text{Fe}_3\text{O}_4$  nanoparticles before coating with silver shell. The  $\text{Fe}_3\text{O}_4$  have a mean diameter of 50 nm and aggregated together [Fig. 2(b)]. In contrast, the  $\text{Fe}_3\text{O}_4@Ag$  nanoparticles are well-dispersed with the use of surfactant to prevent the nanoparticles from aggregating together [Fig. 2(c)]. Each  $\text{Fe}_3\text{O}_4@Ag$  nanoparticles has a mean diameter of about 140 nm [Fig. 2(d)].

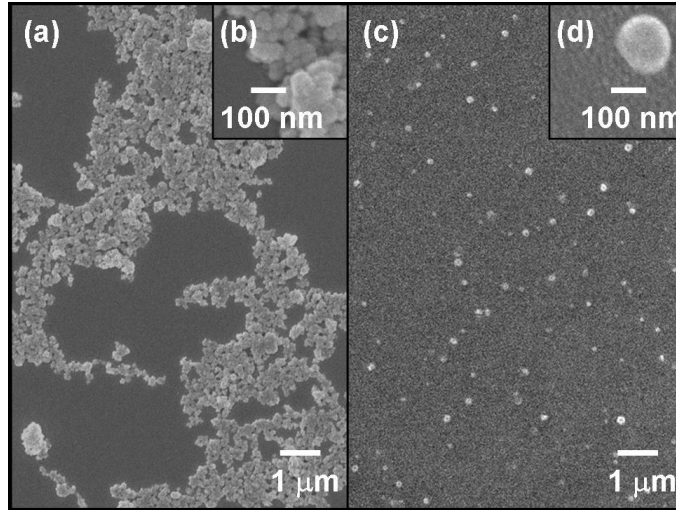


Figure 2. (a) FESEM and (b) zoomed in FESEM image of raw  $\text{Fe}_3\text{O}_4$  nanoparticles. (c) FESEM and (d) zoomed in FESEM image of  $\text{Fe}_3\text{O}_4@Ag$  nanoparticles.

Figure 3 illustrates the magnetic  $\text{Fe}_3\text{O}_4@Ag$  nanoparticles suspended in a solution (a) without and (b) with the influence of an external magnet. Without an external magnet [Fig. 3(a)], the magnetic  $\text{Fe}_3\text{O}_4@Ag$  nanoparticles are suspended in the solution, giving a uniform color. On the contrary, these magnetic nanoparticles are attracted to the external magnet to render a clear solution on the side of the vial without the influence of a magnet [Fig. 3(b)].

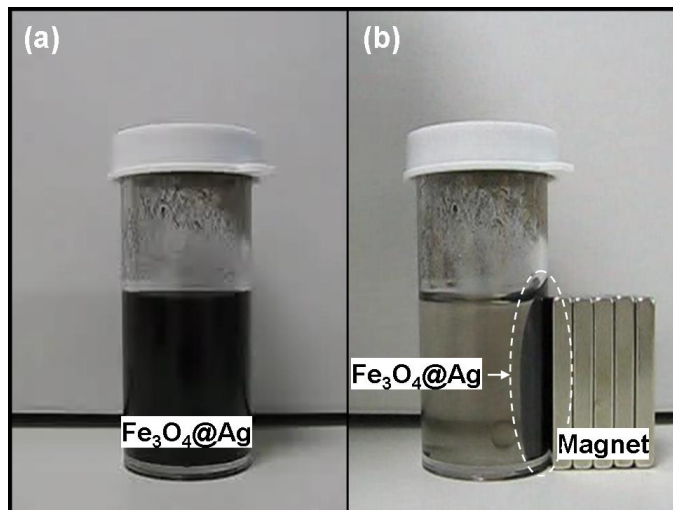


Figure 3. (a)  $\text{Fe}_3\text{O}_4@Ag$  nanoparticles and (b) attracted to the wall of vial in a solution next to an external magnet.

Figure 4 shows the SERS spectra of aqueous R6G solution at concentrations ranging from  $10^{-6}$  M to  $10^{-9}$  M adsorbed on the fabricated  $\text{Fe}_3\text{O}_4@\text{Ag}$  nanoparticles. Prominent Raman peaks, such as C – C – C ring in-plane bending ( $611\text{ cm}^{-1}$ ), CH out-of-plane bending ( $772\text{ cm}^{-1}$ ), C – O – C stretching ( $1181\text{ cm}^{-1}$ ), C – C/ C – N stretching ( $1308$  and  $1360\text{ cm}^{-1}$ ), and aromatic C – C stretching (at  $1507\text{ cm}^{-1}$ ),<sup>12</sup> can be clearly observed in the SERS spectra of R6G adsorbed on the  $\text{Fe}_3\text{O}_4@\text{Ag}$  nanoparticles. These results demonstrates that the fabricated SERS-active nanoparticles are effective in the sensitive detection of chemical test molecules and thus, the sensitive detection of biocrystals,  $\beta$  – hematin, at low concentrations could also be feasible with the use of these  $\text{Fe}_3\text{O}_4@\text{Ag}$  nanoparticles.

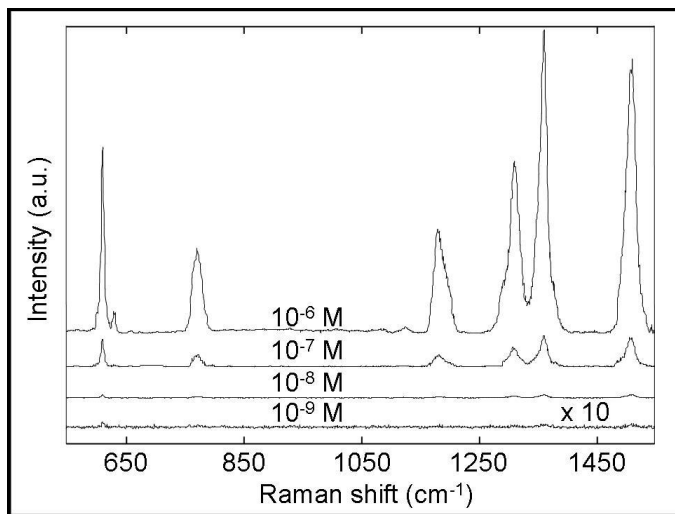


Figure 4. SERS spectra of R6G at a range of concentrations ( $10^{-6}$  to  $10^{-9}$  M) adsorbed on  $\text{Fe}_3\text{O}_4@\text{Ag}$  nanoparticles. The SERS spectrum of R6G at concentration  $10^{-9}$  M is scaled by a factor of 10 for the purpose of comparison.

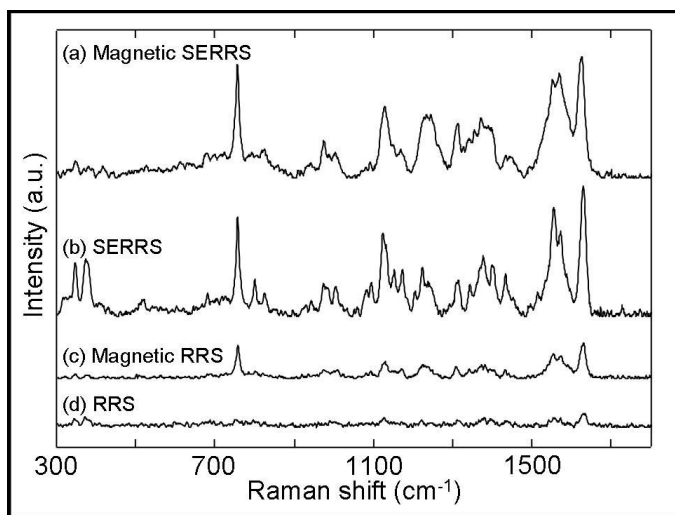


Figure 5. (a) Magnetic field-enriched SERRS spectrum of  $\beta$  – hematin (concentrations of  $10^{-7}$  M). (b) SERRS spectrum of  $\beta$  – hematin (concentrations of  $10^{-5}$  M). (c) Magnetic field-enriched RRS spectrum of  $\beta$  – hematin (concentrations of  $10^{-6}$  M). (d) RRS spectrum of  $\beta$  – hematin (concentrations of  $10^{-4}$  M). The excitation power was 0.1 mW for SERRS spectra and 10 mW for RRS spectra.

Figure 5 shows the (a) magnetic field-enriched SERRS spectrum, (b) SERRS spectrum, (c) magnetic field-enriched RRS spectrum, and (d) RRS spectrum of  $\beta$ -hematin. Prominent Raman peaks, such as  $\nu_8$  ( $345\text{ cm}^{-1}$ , based on the tetragonal  $D_{4h}$  system electron spin and crystallographic coordination notation for resonance Raman peaks studies on myoglobin),<sup>13</sup>  $\gamma_6$  ( $367\text{ cm}^{-1}$ ),  $\nu_{15}$  ( $754\text{ cm}^{-1}$ ),  $\nu_{22}$  ( $1120\text{ cm}^{-1}$ ),  $\nu_{11}$  ( $1551\text{ cm}^{-1}$ ),  $\nu_2$  ( $1570\text{ cm}^{-1}$ ), and  $\nu_{10}$  ( $1628\text{ cm}^{-1}$ ),<sup>14</sup> are observed in these spectra of  $\beta$ -hematin. Among the four different strategies, the magnetic field-enhanced SERRS measurement is the most effective, although low  $\beta$ -hematin concentration of  $10^{-7}\text{ M}$  and laser excitation power of  $0.1\text{ mW}$  has been used. Therefore, the descending order of detection sensitivity for the four different strategies is magnetic field-enriched SERRS, SERRS, magnetic field-enriched RRS, and RRS. More details of this study can be found in a paper in press.<sup>15</sup>

## 4. CONCLUSIONS

In conclusion, the magnetic field-enriched SERRS strategy can enhance the Raman signal of  $\beta$ -hematin using  $\text{Fe}_3\text{O}_4@Ag$  nanoparticles under the influence of a magnetic field. This strategy shows promises for the early diagnosis of malaria disease.

## ACKNOWLEDGEMENTS

This research was funded by the Bill and Melinda Gates Foundation through the Grand Challenges Explorations Initiative (Grant No. OPP1015169).

## REFERENCES

- [1] World Health Organization, "World malaria report 2010," (2010).
- [2] Crawley, J., Chu, C., Mtove, G., and Nosten, F., "Malaria in children," *Lancet* 375, 1468-1481 (2010).
- [3] Froch, T., Koncareyic, S., Zedler, L., Schmitt, M., Schenzel, K., Becker, K., and Popp, J., "In situ localization and structural analysis of the malaria pigment hemozoin," *J. Phys. Chem. B* 111, 11047-11056 (2007).
- [4] Murray, C. K., Gasser, R. A., Magill, A. J., and Miller, R. S., "Update on rapid diagnostic testing for malaria," *Clin. Microbiol. Rev.* 21, 97-110 (2008).
- [5] Liu, Q., and Yuen, C., "Effect of magnetic field in malaria diagnosis using magnetic nanoparticles," *Proc. SPIE*. 8087, 80870E (2011).
- [6] Serebrennikova, Y. M., Patel, J., and Garcia-Rubio, L. H., "Interpretation of ultraviolet-visible spectra of malaria parasite plasmodium falciparum," *Appl. Opt.* 49, 180-188 (2010).
- [7] Bohle, D. S., Conklin, B. J., Cox, D., Madsen, S. K., Paulson, S., Stephens, P. W., and Yee, G. T., "Structural and spectroscopic studies of  $\beta$ -hematin (the heme coordination polymer in malaria pigment)," *ACS Symp. Ser.* 572, 497-515 (1994).
- [8] Zhai, Y., Zhai, J., Wang, Y., Guo, S., Ran, W., and Dong, S., "Fabrication of iron oxide core/gold shell submicrometer spheres with nanoscale surface roughness for efficient surface-enhanced Raman scattering," *J. Phys. Chem. C* 113, 7009-7014 (2009).
- [9] Charan, S., Kuo, C. W., Kuo, Y., Singh, N., Drake, P., Lin, Y. J., Tay, L., and Chen, P., "Synthesis of surface enhanced Raman scattering active magnetic nanoparticles for cell labeling and sorting," *J. Appl. Phys.* 105, 07B310 (2009).
- [10] Egan, T. J., Mavuso, W. W., and Ncokezi, K. K., "The mechanism of  $\beta$ -hematin formation in acetate solution. Parallels between hemozoin formation and biomineralization," *Biochemistry* 40, 204-213 (2001).
- [11] Noland, G. S., Briones, N., and Sullivan, D. J., "The shape and size of hemozoin crystals distinguishes diverse Plasmodium species," *Mol. Biochem. Parasitol.* 130, 91-99 (2003).
- [12] Yuen, C., Zheng, W., and Huang, Z., "Improving surface-enhanced Raman scattering effect using gold-coated hierarchical polystyrene bead substrates modified with postgrowth microwave treatment," *J. Biomed. Opt.* 13, 064040 (2008).
- [13] Hu, S., Smith, K. M., and Spiro, T. G., "Assignment of protoheme resonance Raman spectrum by heme labeling in myoglobin," *J. Am. Chem. Soc.* 118, 12638-12646, (1996).

- [14] Wood, B. R., Langford, S. J., Cooke, B. M., Lim, J., Glenister, F. K., Duriske, M., Unthank, J. K., and McNaughton, D., "Raman spectroscopy reveals new insight into the electronics structure of  $\beta$  – hematin and malaria pigment," *J. Am. Chem. Soc.* 126, 9233-9239 (2004).
- [15] Yuen, C., and Liu, Q., "Magnetic field enriched surface enhanced resonance Raman spectroscopy for early malaria diagnosis," *J. Biomed. Opt.* (in press).